Russian Federal Nuclear Center

All-Russian Scientific Research Institute of
Experimental Physics

APPROVED BY

Deputy Scientific Leader

V.N.Mokhov

1995 г.

**STUDYING POSSIBILITY OF X RADIATION GENERATION AT LOW –
DENSE PLASMA COMPRESSION USING HIGH – POWER EMG.**

(Final report under subcontract
F 6170894W0757)

JPC-94-4076

19980303 139

DTIC QUALITY INSPECTED 3

607200 Arzamas-16, Nizhny Novgorod region., RF.
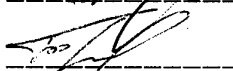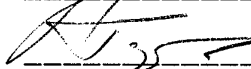
1995

REPORT DOCUMENTATION PAGE

Form Approved OMB No. 0704-0188

1. AGENCY USE ONLY (Leave blank)	2. REPORT DATE	3. REPORT TYPE AND DATES COVERED
	1995	Final Report

4. TITLE AND SUBTITLE

Studying Possibility of X Radiation Generation at Low - Dense Plasma Compression Using High Power EMG

5. FUNDING NUMBERS

F6170894W0758

6. AUTHOR(S)

Prof. Vladislav Mokhov

7. PERFORMING ORGANIZATION NAME(S) AND ADDRESS(ES)

Institute of Experimental Physics
Prospekt Mira 37
Arzamas-16 Russia
Russia

8. PERFORMING ORGANIZATION REPORT NUMBER

N/A

9. SPONSORING/MONITORING AGENCY NAME(S) AND ADDRESS(ES)

EOARD
PSC 802 BOX 14
FPO 09499-0200

10. SPONSORING/MONITORING AGENCY REPORT NUMBER

SPC 94-4076

11. SUPPLEMENTARY NOTES

12a. DISTRIBUTION/AVAILABILITY STATEMENT

Approved for public release; distribution is unlimited.

12b. DISTRIBUTION CODE

A

13. ABSTRACT (Maximum 200 words)

This report results from a contract tasking Institute of Experimental Physics as follows: Consider the physical scheme of an arrangement for x-ray generation by quasi-spherical compression based on theoretical analysis and 1D calculations as described in the proposal dated 8-Aug-94.

14. SUBJECT TERMS

Nil

15. NUMBER OF PAGES

34

16. PRICE CODE

N/A

17. SECURITY CLASSIFICATION OF REPORT	18. SECURITY CLASSIFICATION OF THIS PAGE	19, SECURITY CLASSIFICATION OF ABSTRACT	20. LIMITATION OF ABSTRACT
UNCLASSIFIED	UNCLASSIFIED	UNCLASSIFIED	UL

NSN 7540-01-280-5500

Standard Form 298 (Rev. 2-89)
Prescribed by ANSI Std. 239-18
298-102

INVESTIGATORS

_____ A. M. Buyko

_____ O. M. Burenkov

_____ S. F Garanin

_____ V. F. Yermolovich

_____ V. N. Mokhov

_____ A. I. Startsev

_____ A. I. Sushko

_____ V. B. Yakubov

Table of Contents.

1. Introduction.

This report considers capabilities of the system with compression of low – dense plasma heated to temperature $T_0 \cong 0.1 \div 0.3\ keV$ with a relatively slow liner ($V_0 \cong 1 \div 3\ cm/\mu s$) to obtain megajoule amounts of X radiation.

The report does not consider a specific facility design, issues of plasma pre – heating and radiation withdrawal. At this stage the principal objective is to find out possible values of the system parameters basing on estimations, analytic and one – dimensional numerical computations which will allow to consider the issue whether or not it is reasonable to develop this direction of research.

2. Selection of physical scheme.

Selection of the physical scheme with quasi – spherical plasma compression with a liner was discussed in the first part of the report [%]. It is assumed that quasi – spherical (not necessarily hydrogen) plasma compression can be made using a system similar to that intended for reachment of DT – plasma ignition threshold at plasma chamber compression by a liner.

We will consider a system where kinetical energy of the spherical shell is converted to X radiation energy at implosion of intermediate "working substance", i. e. plasma, heated to temperature $T_0 = 0.2$ keV at the initial spherical shell radius of $R_0 = 6$ cm. Such selection of initial plasma parameters prior to discussion of a pre – heating technique is arbitrary to some extent. We oriented to typical plasma parameters in the MAGO system chamber which can be considered as one of possible pre – heating variants.

In our computation initial kinetic energy of the shell was selected equal to $E_0 = 20$ MJ which corresponds to capabilities of appropriate EMG.

The report presents similarity parameters allowing to update basic system characteristics for other initial conditions. Initial plasma density and shell velocity were selected so that maximum plasma temperature be reached at compression $\delta = \rho/\rho_0 \leq 1000$ which seems to be quite real for spherical systems since shell radius will vary no more than by a factor of 10. Reachment of high compressions will be impeded with shell motion instability. The possibility to obtain X radiation with quanta energy of $h\nu \sim 5 \div 10$ keV at shell velocity of $V_0 \sim 3 \div 5$ $cm/\mu s$ is based on absence of radiation – material equilibrium due to low plasma density. For low – z plasma at temperature $\sim 5 \div 10$ keV the basic radiation mechanism is bremsstrahlung. Thus, the system under consideration must be bremsstrahlung spectrum X radiation source with characteristic emission time $\tau \cong 0.1 \dfrac{R_0}{V_0} \approx 0.2$ μs.

3. Zero – dimensional computation setting – up and results.

3.1 Computations without account of compressing shell deceleration.

To find out principal features of the processes under consideration, treat the problem of adiabatic compression of plasma heated to initial temperature T_0 by a shell moving at constant velocity V_0. Plasma is assumed to be fully ionized and low – dense, i.e. there is no radiation – material equilibrium owing to very low optical thickness of plasma under consideration. Assume that plasma energy losses to radiation are described by the formula for bremsstrahlung [2]

$$q = 1.97 \cdot 10^5 \cdot \rho \frac{z^3}{A^2} \sqrt{T_e} \quad [MJ/g \cdot \mu s] \tag{3.1}$$

where ρ – plasma density $[g/cm^3]$,

T_e – electron temperature $[keV]$,

z – ion charge,

A – atomic weight.

Write energy balance for electron and ion plasma components (per $1g$ of material) in the form:

$$\frac{d\varepsilon_i}{dt} = -P_i \frac{d\rho^{-1}}{dt} - c_i \frac{(T_i - T_e)}{\tau_{ie}} \tag{3.2}$$

$$\frac{d\varepsilon_e}{dt} = -P_e \frac{d\rho^{-1}}{dt} + c_i \frac{(T_i - T_e)}{\tau_{ie}} - q \tag{3.3}$$

Here:

$\varepsilon_i = c_i T_i$ – internal energy of the ion component,

$\varepsilon_e = zc_i T_e$ – internal energy of the electron component,

$P_i = \frac{2}{3} c_i \rho T_i$ – ion pressure,

$P_e = \frac{2}{3} zc_i \rho T_e$ – electron pressure,

c_i – plasma ion component heat capacity,

τ_{ie} – electron and ion temperature smoothing time,

q – deceleration energy losses.

If temperature smoothing time is much less than compressing characteristic times $\left(\tau_{ie} \ll \tau = \dfrac{R_0}{V_0} \right)$ then the adiabaticity condition is satisfied for the equation system 3.2, 3.3 which can be written in the form

$$T_i - T_e \approx \frac{q\,\tau_{ie}}{(z+1)c_i} \tag{3.4}$$

In this case the equation system reduces to the equation

$$\frac{d}{dt}\left(\frac{T_e}{\rho^{2/3}} \right) = -\frac{q}{\rho^{2/3} c_i (z+1)} \tag{3.5}$$

Introduce the following notations:

ρ_0 – initial plasma density,

T_0 – initial plasma temperature,

$\delta \equiv \dfrac{\rho}{\rho_0}$ – (relative density or compression degree of plasma),

$s \equiv \dfrac{T_e}{\rho^{2/3}} \cdot \dfrac{\rho_0^{2/3}}{T_0}$ – a dimensionless value whose logarithm determines electron entropy,

R_0 – initial density radius,

V_0 – shell motion velocity,

$\tau \equiv \dfrac{R_0}{V_0}$ - characteristic compression time.

When shell moves at a constant velocity the compression degree is described with the formula

$$\delta^{\frac{1}{3}} = \frac{\tau}{\tau - t} \tag{3.6}$$

Eq. (3.5) with account of (3.1) and (3.6) reduces to the dimensionless form

$$\frac{d\sqrt{s}}{d\delta} = -a\delta^{-2/3} \tag{3.7}$$

where

$$a = \frac{224.5 R_0 \rho_0 z^3}{V_0 \sqrt{T_0}\, A(z+1)} \tag{3.8}$$

The solution of Eq. (3.7) is of the form

$$s = \left(1 + 3a\right)^2 \left(1 - \frac{3a}{1 + 3a}\, \delta^{1/3}\right)^2 \tag{3.9}$$

From this expression it is seen that when compression

$$\delta_* = \left(\frac{1 + 3a}{3a}\right)^3 \tag{3.10}$$

is reached plasma temperature vanishes. The corresponding time is

$$t_* = \tau \cdot \frac{\delta_*^{1/3} - 1}{\delta_*^{1/3}} \tag{3.11}$$

Using formulas (3.6), (3.10), (3.11) one can represent (3.9) in the form

$$s(\delta) = \frac{\delta_*^{2/3}}{\delta_*^{2/3} - 1}\left(1 - \left(\frac{\delta}{\delta_*}\right)^{1/3}\right)^2 \tag{3.12 a}$$

or

$$s(t) = \frac{\tau^2}{t_*^2}\left(\frac{t_*}{\tau - t} - t\right)^2. \tag{3.12 b}$$

Plasma density, temperature and pressure are described by the formulas

$$\rho = \rho_0 \delta = \rho_0 \frac{\tau^3}{\left(\tau - t\right)^3}, \tag{3.13}$$

$$T = T_0 \delta^{2/3} s(\delta) = T_0 \frac{\tau^2}{\left(\tau - t\right)^2} \cdot s(t , \tag{3.14}$$

$$P^{\cdot} = P_0 \delta^{2/3} s(\delta) = P_0 \frac{\tau^5}{\left(\tau - t\right)^5} \cdot s(t), \tag{3.15}$$

where $P_0 = \frac{2}{3}(z + 1)c_i \rho_0 T_0$ – initial plasma pressure..

Plasma energy is

$$E = (z + 1)c_i T \frac{4\pi}{3}\rho_0 R_0^3$$

or

$$E = E_0 \delta^{2/3} \cdot s(\delta) = E_0 \frac{\tau^2}{(\tau - t)^2} s(t) \qquad (3.16)$$

where E_0 – initial plasma energy.

The work of entire plasma compression per time unit is of the form

$$\dot{A} = \frac{2E_0}{\tau} \delta \cdot s(\delta) = 2E_0 \frac{\tau^2}{(\tau - t)^3} s(t) \qquad (3.17)$$

Intensity of plasma radiation from the whole compressed volume is

$$\dot{Q} = \frac{2E_0}{\tau} \frac{\delta^{4/3} - s^{1/2}(\delta)}{\delta_*^{1/3} - 1} = 2E_0 \frac{(\tau - t_*)}{t_*} \cdot \frac{\tau^3}{(\tau - t)^4} \cdot s^{1/2}(t) \quad (3.18)$$

The integral values corresponding to (3.17) and (3.18) (shell work on plasma and radiation energy released from plasma) are described by formulas

$$A(\delta) = E_0 \cdot \frac{\delta_*^{2/3}}{(\delta_*^{1/3} - 1)^2} \left[(\delta^{2/3} - 1) - \frac{4}{3\delta_*^{1/3}} (\delta - 1) + \frac{1}{2\delta_*^{2/3}} (\delta^{4/3} - 1) \right] \quad (3.19)$$

and

$$Q(\delta) = E_0 \cdot \frac{\delta_*^{2/3}}{(\delta_*^{1/3} - 1)^2} \left[\frac{2}{3\delta_*^{1/3}} (\delta - 1) - \frac{1}{2\delta_*^{2/3}} (\delta^{4/3} - 1) \right]. \qquad (3.20)$$

Using formulas (3.15) – (3.18) one can obtain an expression for maximum values of plasma parameters: *)
maximum temperature

$$\max T \approx 0.0625 T_0 \cdot \delta_*^{2/3} \qquad (3.21)$$

is reached at $\delta = 0.125\delta_*$;
maximum work flow

$$\max \dot{A} \approx 0.691 \frac{E_0}{\tau} \delta_*$$

is reached at $\delta = 0.216\delta_*$;
maximum radiation intensity

$$\max \dot{Q} \approx 0.164 \frac{E_0}{\tau} \delta_* \qquad (3.22)$$

---

*) In the approximate formulas given below it is assumed that $\delta_*^{1/3} \gg 1$.

is reached at $\delta = 0.512\delta_*$.

From formulas (3.19), (3.20) one can derive expression for limiting values of work done on plasma and emitted energy(at the time when $\delta = \delta_*$)

$$A_* \approx Q_* \approx \frac{E_0}{6}\delta_*^{2/3} \qquad (3.23)$$

Figs. 3.1 and 3.2 give plots illustrating formulas (3.14) – (3.20). In the selected scales the plots are of universal character and practically do not depend on particular value of the parameter δ_*. Temperature was therewith normalized to $\max T$, differential works and radiations to $\max \dot{Q}$, integral works and radiation flows and plasma energy to $A(\delta_*)$.

Basic values vs plasma compression degree
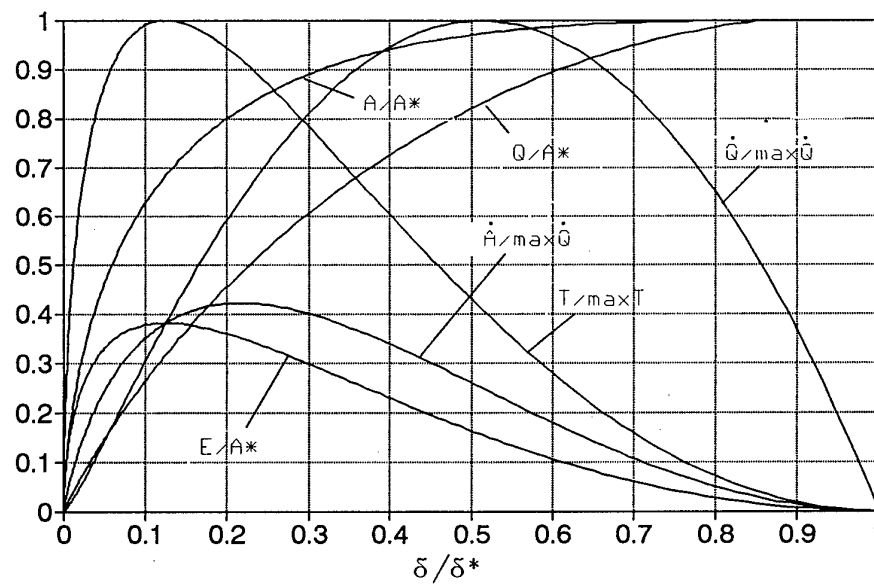when sell moves at constant velocity.

Fig. 3. 1

Basic values vs time when shell moves at
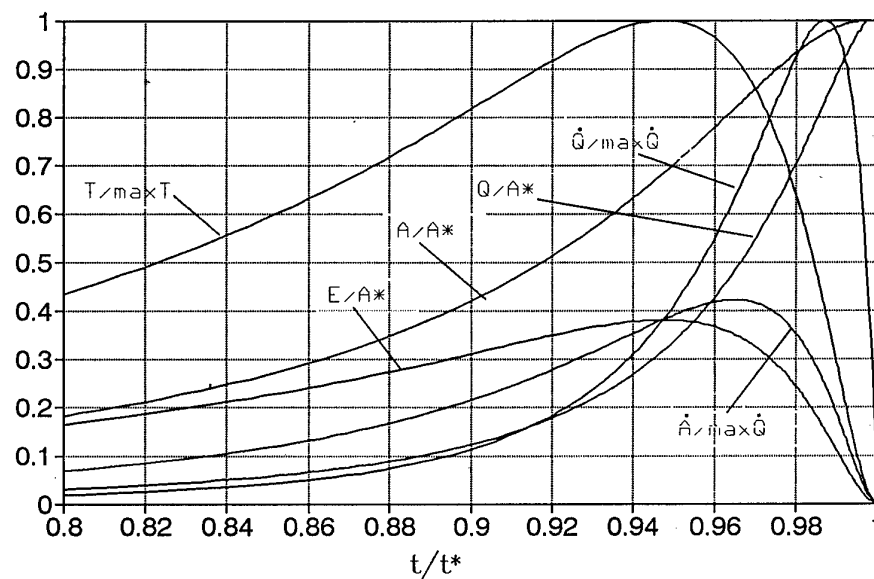constant velocity.

Fig. 3. 2

The principal feature of the obtained solution is that beginning from certain time plasma radiation intensity becomes higher than work flow at the boundary and plasma begins to cool dramatically. In so doing, irrespective of infinite shell energy (absence of deceleration) finite work (3.23) is being done on plasma. The X radiation pulse has a stretched leading and very steep back front (Fig. 3.2). Maximum radiation intensity is reached when plasma compression is 4 times higher than at maximum temperature, plasma temperature being reduced down to $T \cong 0.4 \max T$.

Consider some quantitative estimations. Assuming that plasma compression by the shell is constant up to $\delta \cong 1000$, select $\delta_* = 8000$, then, according to (3.21), at $\delta \cong 1000$ maximum temperature $T \approx 25 T_0$, internal plasma energy $E \approx 25 E_0$, differential work flow $\overset{\bullet}{A} \cong 500 \dfrac{E_0}{\tau}$, radiation intensity $\overset{\bullet}{Q} \cong 500 \dfrac{E_0}{\tau}$ are reached. By that time plasma emits energy $Q = 21 E_0$, while the ultimate value of emitted energy, according to (3.23), is $Q_* = 67 E_0$. Maximum work flow is reached at $\delta = 1720$ and is $\overset{\bullet}{A} \cong 550 \dfrac{E_0}{\tau}$, at that time radiation intensity is $\overset{\bullet}{Q} \cong 830 \dfrac{E_0}{\tau}$ at temperature $T \cong 23 T_0$. By that time energy $Q \cong 32 E_0$ is emitted. Maximum radiation intensity $\overset{\bullet}{Q} \cong 1300 \dfrac{E_0}{\tau}$ is reached at compression $\delta \cong 4000$, at temperature $T \cong 10 T_0$. By that time energy $Q \cong 55 E_0$ is emitted.

3.2 Computations with account of compressing shell deceleration.

To account shell acceleration, complete Eq. (3.5) with the equation of shell motion

$$m \frac{dV}{dt} = -4\pi R^2 P, \qquad (3.24)$$

where m – shell mass, V – shell velocity. Introduce dimensionless velocity $u = \dfrac{V}{V_0}$ and two dimensionless parameters $\chi = 1 - \sqrt{s}$ and $k = \dfrac{E_0}{W_0}$ where $W_0 \equiv \dfrac{mV_0^2}{2}$ – initial shell energy. Transform Eq. (3.5) to the form

$$\frac{dt}{d\chi} = \frac{\tau}{3a\delta^{2/3}}. \qquad (3.25)$$

Eq. (3.24) with account of (3.25) is reduced to the form

$$\frac{du}{d\chi} = -\frac{k}{3a} \delta^{1/3} (1 - \chi)^2 \qquad (3.26)$$

Formula (3.6) has to be replaced with the equation

$$\frac{d\delta^{1/3}}{d\chi} = \frac{u}{3a}$$ (3.27)

Equation system (3.26), (3.27) yields the parametric solution to the problem and Eq. (3.25) sets correlation of the parameter χ to real time. This equation system is equivalent to the second – order linear equation

$$\frac{d^2\delta^{1/3}}{d\chi^2} + \frac{k}{9a^2}\left(1-\chi\right)^2\delta^{1/3} = 0,$$

whence it is seen, that another dimensionless combination of initial parameters which determines the course of the solution is the expression

$$K_e = \frac{E_0}{W_0 \cdot 9a^2} \approx \frac{E_0}{W_0}\cdot\delta_*^{2/3} \approx 6\frac{Q_*}{W_0}$$ (3.28)

Fig. (3.3) gives results of numerical solution to Eqs. (3.26), (3.27) for a set of K_e values at $\delta_* = 8000$. At $K_e \cong 12$ $\left(W_0 \cong 0.5Q_*\right.$ complete shell deceleration takes place at $\chi = 1$. Apparently, in this case the maximum system efficiency factor is realized: entire shell energy is converted to radiation. At lower values of K_e plasma does not have time to extract whole shell energy due to rapid cooling, at high values of K_e plasma does not have time to convert kinetic energy of the shell to radiation. It should be noted, that the parameters $K_e \sim \dfrac{R_0 T_0^2}{m\rho_0}$ does not explicitly depend on initial shell velocity.

Cite the formulas for computation of physical parameters through solution of Eqs. (3.26, 3.27):

$$E = E_0\delta^{1/3}\left(1-\chi\right)^2,$$

$$T = T_0\delta^{2/3}\left(1-\chi\right)^2,$$

$$\dot{Q} = \frac{2E_0\delta^{4/3}\left(1-\chi\right)}{\tau\left(\delta_*^{1/3}-1\right)},$$

$$\dot{A} = \frac{2E_0}{\tau}\delta\left(1-\chi\right)^2 u,$$ (3.29)

$$A = W_0\left(1-u^2\right),$$

$$Q = A + E_0 - E.$$

Figs. 3.4 – 3.7 give plots of these values computed for several values of K_e, with the parameter a being selected so that maximum temperature be reached at $\delta = 1000$. In these plots temperature is given in units T_0, energy and work in units E_0, differential flows in units $\dfrac{E_0}{\tau}$.

Solution of equation system (3. 26), (3. 27)
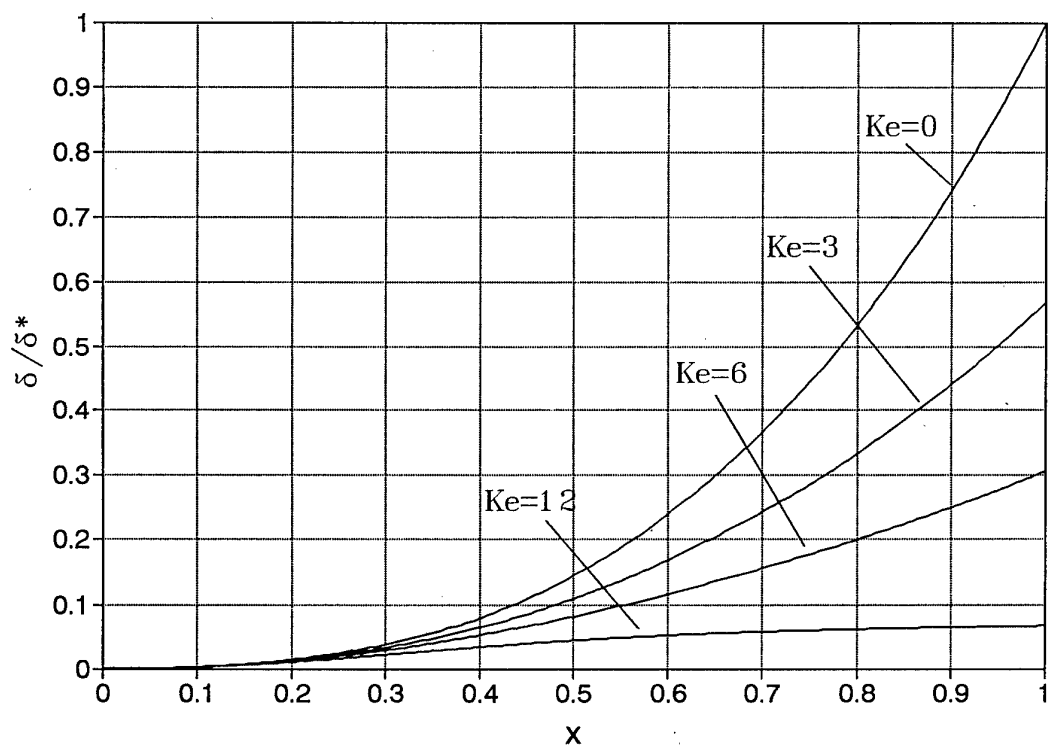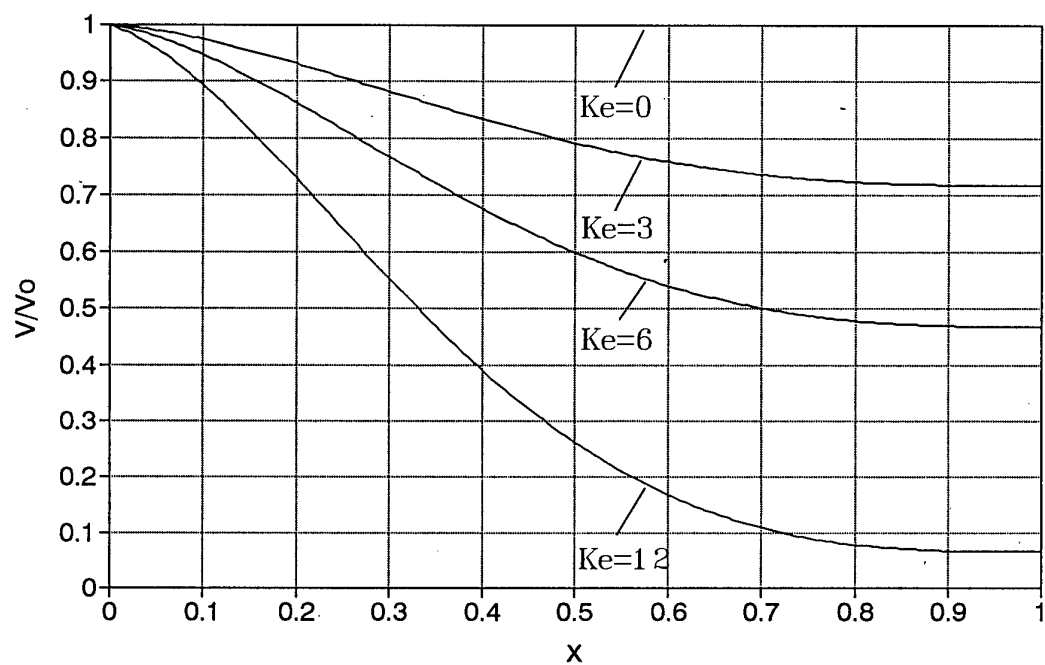for the same values of parameter Ke (δ*=8000)

Fig. 3. 3

Solution of equation system (3.26), (3.27)
for Ke=0.1, δ*=8000.

Fig. 3.4
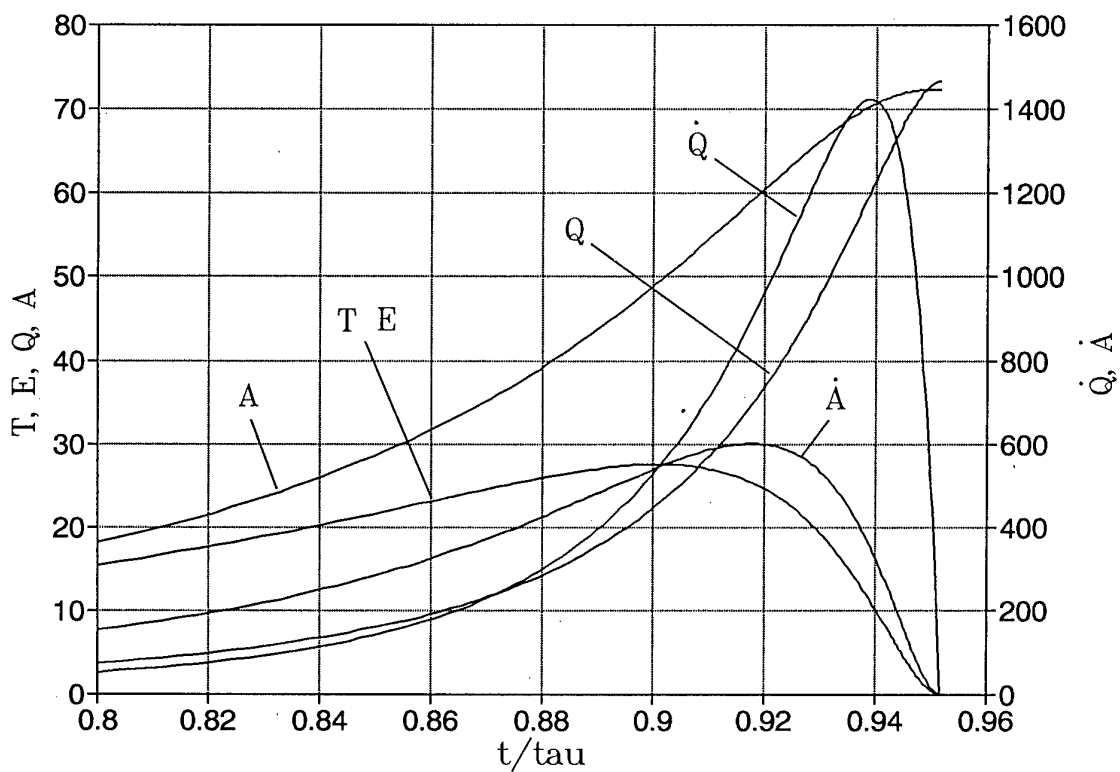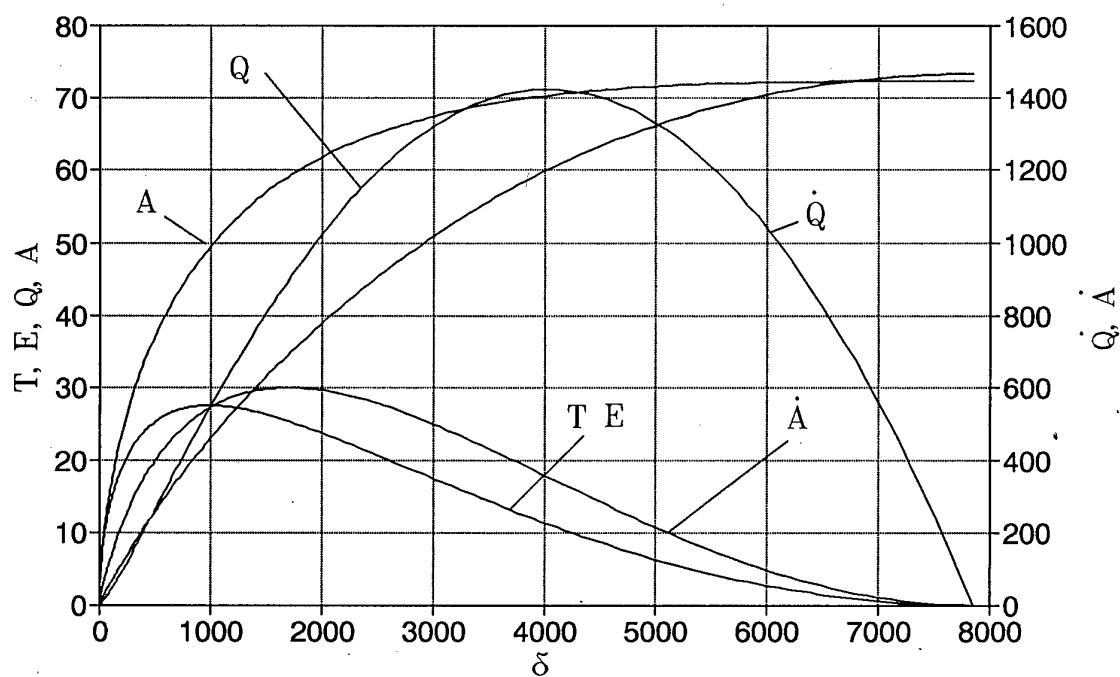
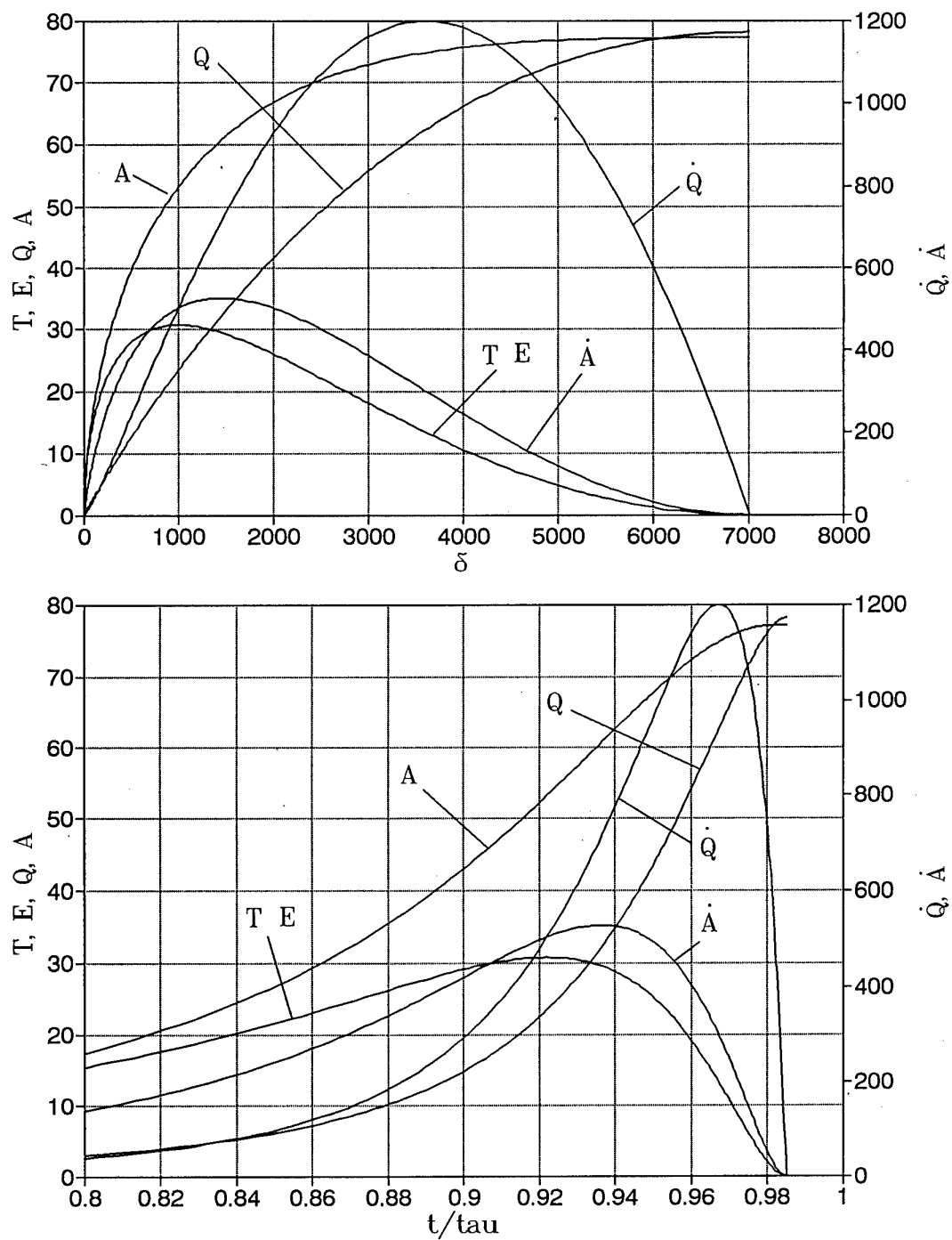Solution of equation system (3. 26), (3. 27)
for Ke=3, δ*=12167

Fig. 3. 5

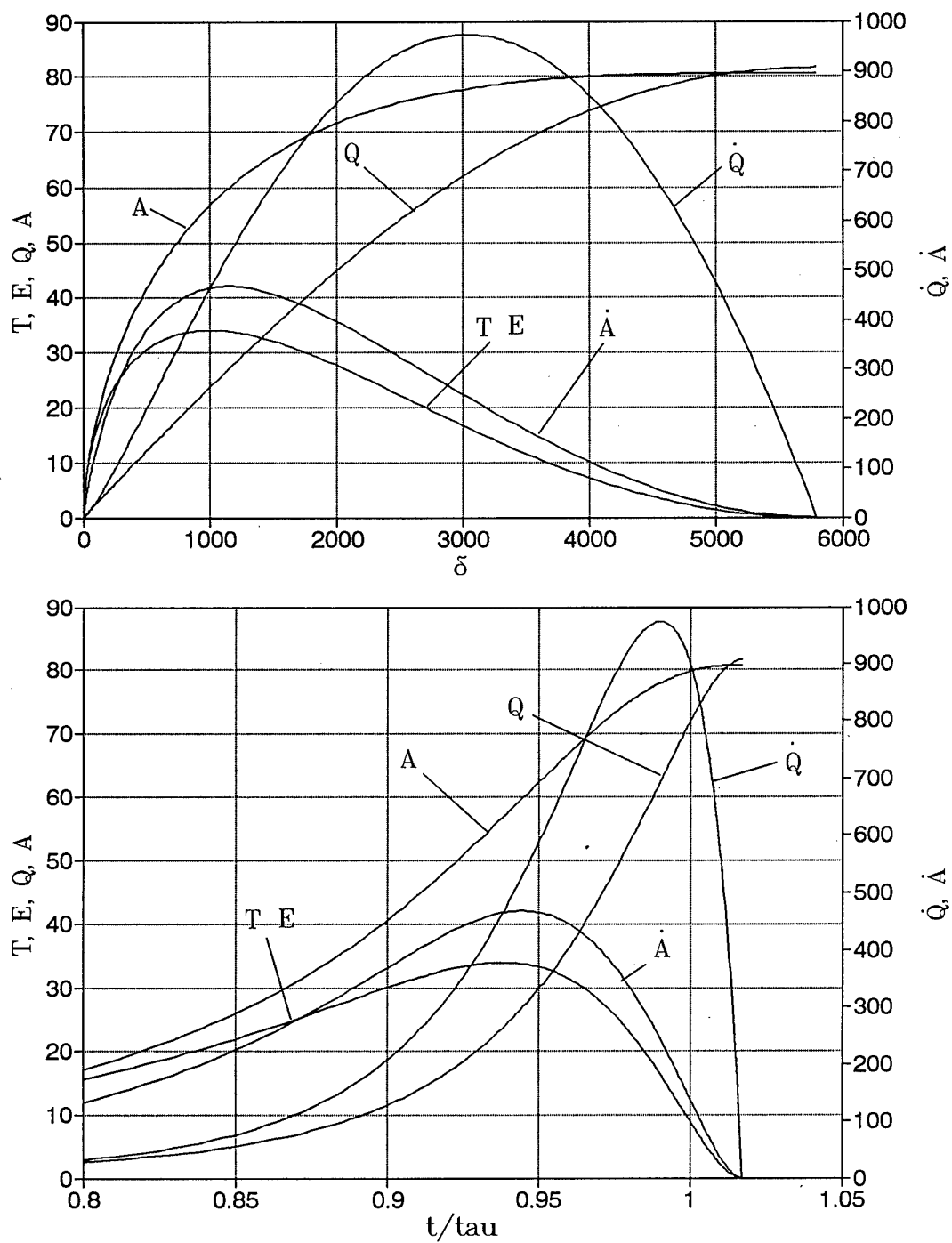Solution of equation system (3. 26) , (3. 27)
for Ke=6, δ*=17985.

Fig. 3. 6

Solution of equation system (3. 26) , (3. 27)
for Ke=12, δ=35288.
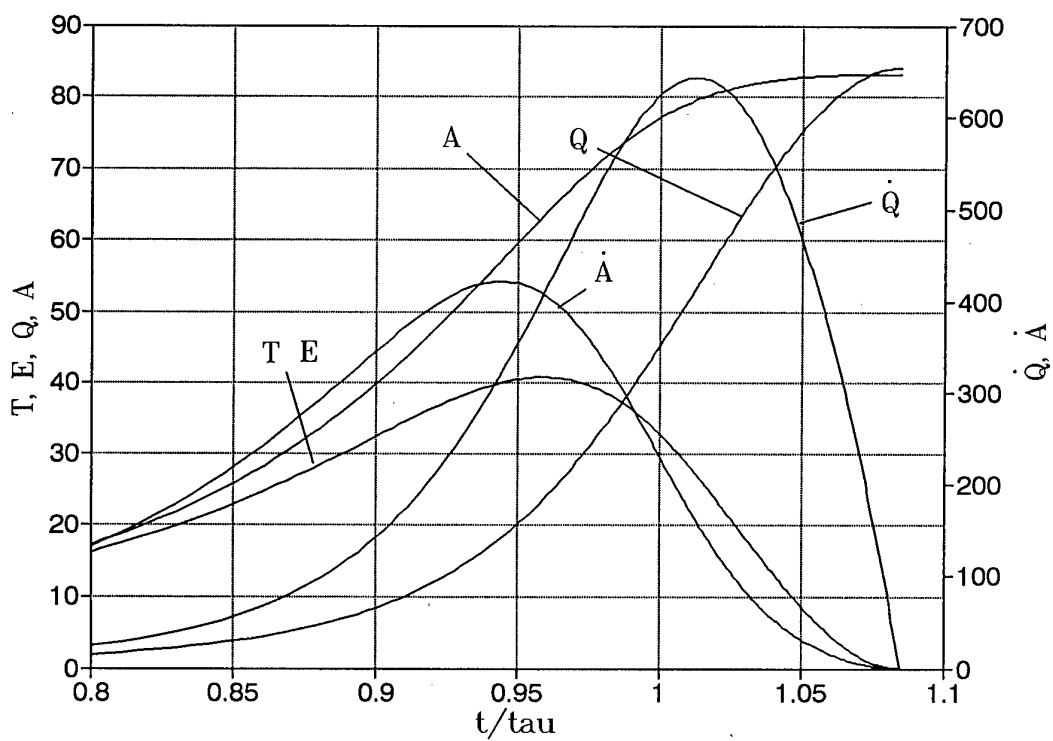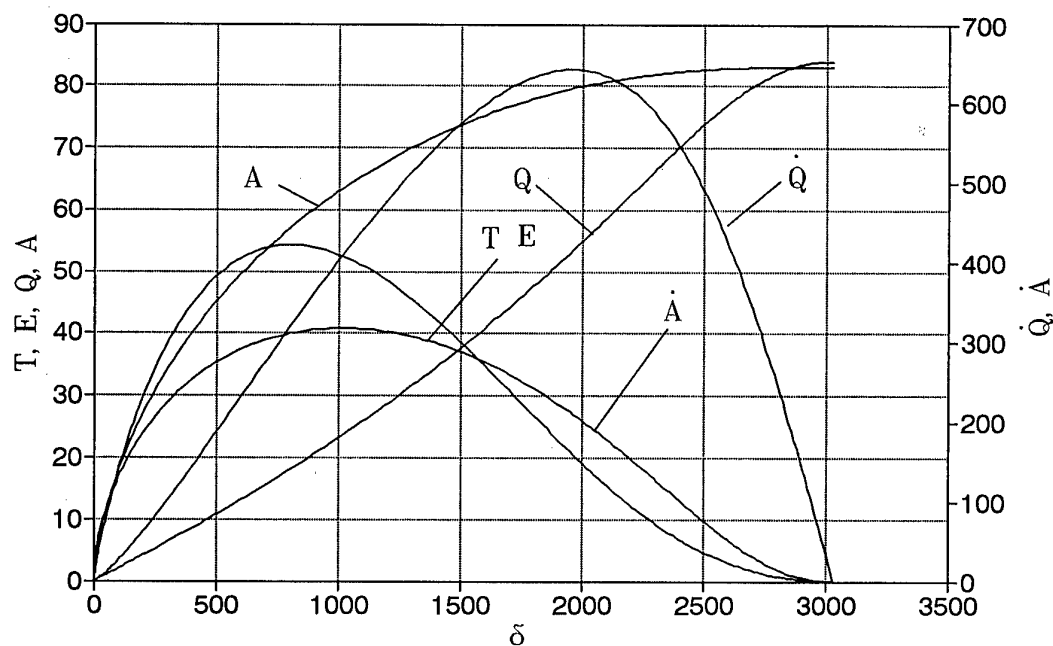

Fig. 3. 7

4. Selection of working material.

The analysis performed in the previous section imposes no explicit limitations on the value z. The limitation on z follows from the applicability condition of formula (3.1) which describes plasma radiation within the temperature range providing not only total material ionization, but also small contribution of bound – free transition radiation. For the initial temperature $T_0 = 0.2\ keV$ only hydrogen and helium satisfy these requirements. Description of high z materials requires specification of the above model. We did it using the interpolation formulas given in paper [3].

With account of energy expenditure on ionization the equation of state of plasma was written in the form

$$P = \frac{2}{3}(z+1)\cdot c_i \cdot \rho \cdot T$$

$$\varepsilon = c_i \cdot (z+1)\cdot T$$

$$c = \frac{d\varepsilon}{dT} = c_i \cdot (z+1) + c_i \cdot T \cdot \frac{dz}{dT} + \frac{dQ_z}{dT}$$

(4.1)

where c_i – heat capacity of ion ideal gas,
$z(T)$ – mean ion charge,
$Q_z(T)$ – expenditure of energy on ionization.

In the approximation accepted in [3] mean ion charge depends only on temperature, in connection with this internal energy and heat capacity of plasma in (4.1) are functions of temperature only. For simplicity the dependency $Q_z(T)$ was taken in the form $Q_z(T) = \alpha\big(z(T)\big)^{7/3}$, with the coefficient α being chosen so that proper energy of total atom ionization be secured.

With account of plasma heat capacity dependence on temperature Eq. (3.5) takes the form

$$\frac{d}{dt}\left(\frac{T}{\rho^{2/3}}\right) = -\frac{2}{3}\cdot\frac{\left(c_i T\dfrac{dz}{dT} + \dfrac{dQ_z}{dT}\right)}{c}\cdot\left(\frac{T}{\rho^{2/3}}\right)\frac{d\rho}{\rho dt} - \frac{q}{c\,\rho^{2/3}}$$

(4.2)

The first addend in the right – hand side accounts consumption of energy on ionization, the second – energy losses on radiation. Instead of formula (3.1) the following expression was used for q

$$q = \rho z(T)\cdot P_z(T),$$

(4.3)

where $z(T)$ and $P_z(T)$ are described by the interpolation formulas from [3]

Eq. (4.2) was numerically solved simultaneously with equations of shell motion (3.24). The initial parameters of the system were selected so that maximum plasma temperature be reached at compression $\delta \approx 1000$ and whole plasma energy be emitted by the time of complete shell deceleration

(the mode with maximum efficiency). The initial shell radius was taken equal to $R_0 = 6\ cm$, the initial shell energy – 20 $W_0 \approx MJ$. The computed results are given in Table 4.1 and in plots of Figs. 4.1 through 4.8.

The computations show that at the initial temperature $T_0 \approx 0.2\ keV$ acceptable results are obtained only for low z (He, Li). As z increases, with the initial temperature being fixed, shell velocity needed to implement the selected mode increases and, accordingly, shell mass decreases. Already for nitrogen ($z = 7$) at $T_0 = 0.2\ keV$ it is impossible to realize the mode with complete shell deceleration at reasonable values of V_0 (see computations Nos. 3,4 in Table 4.1). If maximum temperature is therewith reached at $\delta \approx 1000$, then the mode with low efficiency (~ 10 %) is realized and maximum plasma temperature is too low (computation No. 3, Table 4.1). The complete shell deceleration mode is realized at plasma compression $\delta \approx 2 \cdot 10^4$ (computation No. 4, Table 4.1). It should be noted that transition from mode to mode occurs at relatively small change in initial density.

Computations Nos. 7, 8 of Table 4.1 show that for materials with $z = 7...10$ initial plasma temperature should be $T_0 \approx 0.5...0.9\ keV$.

Mention one more feature of the solution using formula (4.2) for nitrogen and neon. At plasma cooling down to temperature ~1 keV on the dependency $\dot{Q}(t)$ the second acute maximum appears which is related to abrupt increase in energy losses to radiation within this temperature range, but energy emitted in this peak is negligible.

Keeping in mind the possibility to use the MAGO chamber for plasma preheating, we computed the system with the central electrode of 0.1 R_0 (computations Nos. 9, 10 in Table 4.1). Availability of the electrode led to a small decrease in maximum temperature as compared to a similar computation of the system with free center (computation No. 1). Computation No. 11 was performed for comparison with computation No. 7 of Table 5.1.

The computed results show that for "working substance" it is most real to use low z material: helium or even hydrogen. High z materials appear more preferable from the source intensity increase standpoint, but impose more stringent requirements on the initial shell velocity and the initial plasma temperature.

Table 4.1.

| No.	ρ_0 g/cc	V_0 $cm/\mu s$	T_0 keV	m g	$\max T$ keV	$\max \dot{Q}$ $MJ/\mu s$	Q MJ	$\delta_{\max T}$	$\delta_{\max} \dot{Q}$	material
1	$1.3 \cdot 10^{-5}$	3	0.2	45	8.06	71.3	20.3	1029	1798	He
2	$1.75 \cdot 10^{-5}$	6.35	0.2	10	7.72	152	20.1	1045	1873	Li
3	$5.78 \cdot 10^{-6}$	20	0.2	1	1.42	298	1.86	1054	3237	N
4	$4.34 \cdot 10^{-6}$	20	0.2	1	29.6	1170	18.8	$2 \cdot 10^4$	$3.6 \cdot 10^4$	N
5	$5 \cdot 10^{-6}$	0.707	0.5	800	20.86	15.84	20	1015	1716	He
6	$6.6 \cdot 10^{-6}$	1.41	0.5	200	20.61	31.04	20	1019	1703	Li
7	$7.6 \cdot 10^{-6}$	6.35	0.5	10	16.2	166	19.3	1086	2779	N
8	$4.8 \cdot 10^{-6}$	4.7	0.9	18.5	26.72	177.7	20.1	1024	2436	Ne
9	$1.5 \cdot 10^{-5}$	2.5	0.2	64	6.3	95.2	20	1051	2051	He
10	$1.3 \cdot 10^{-5}$	3	0.2	45	9.8	77	16.8	1307	1554	He
11	$1.3 \cdot 10^{-5}$	3.5	0.2	33	9.2	67.1	19.6	1052	1464	He

Results of computation 1 from Table 4. 1
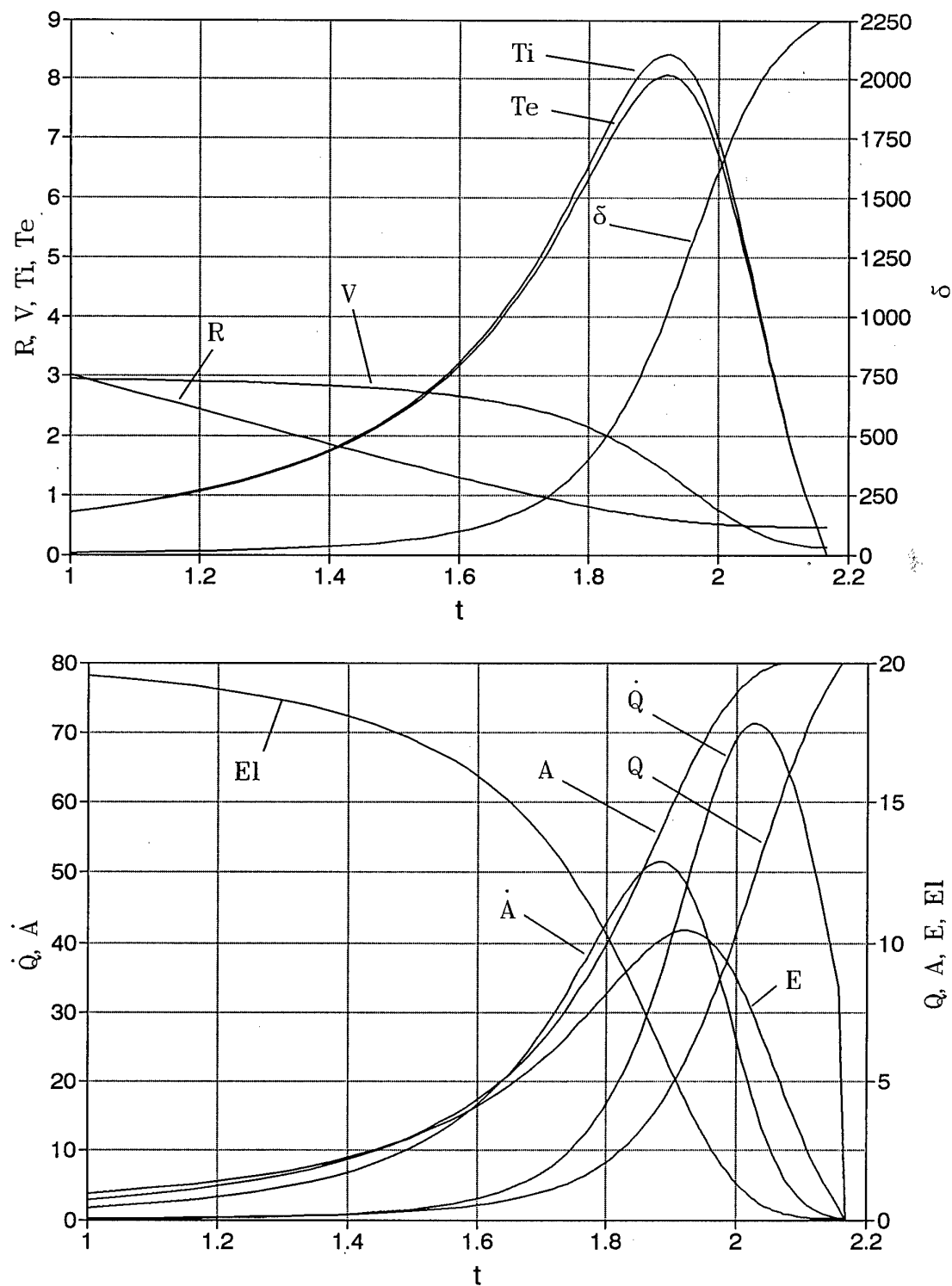
Fig. 4. 1

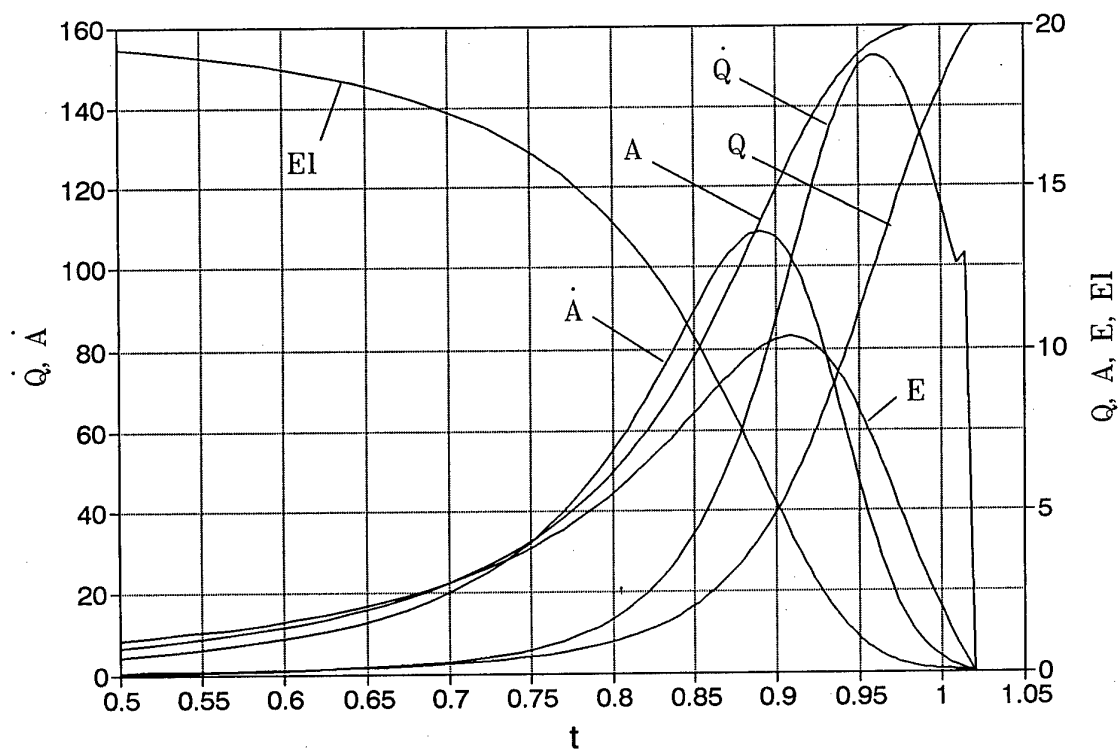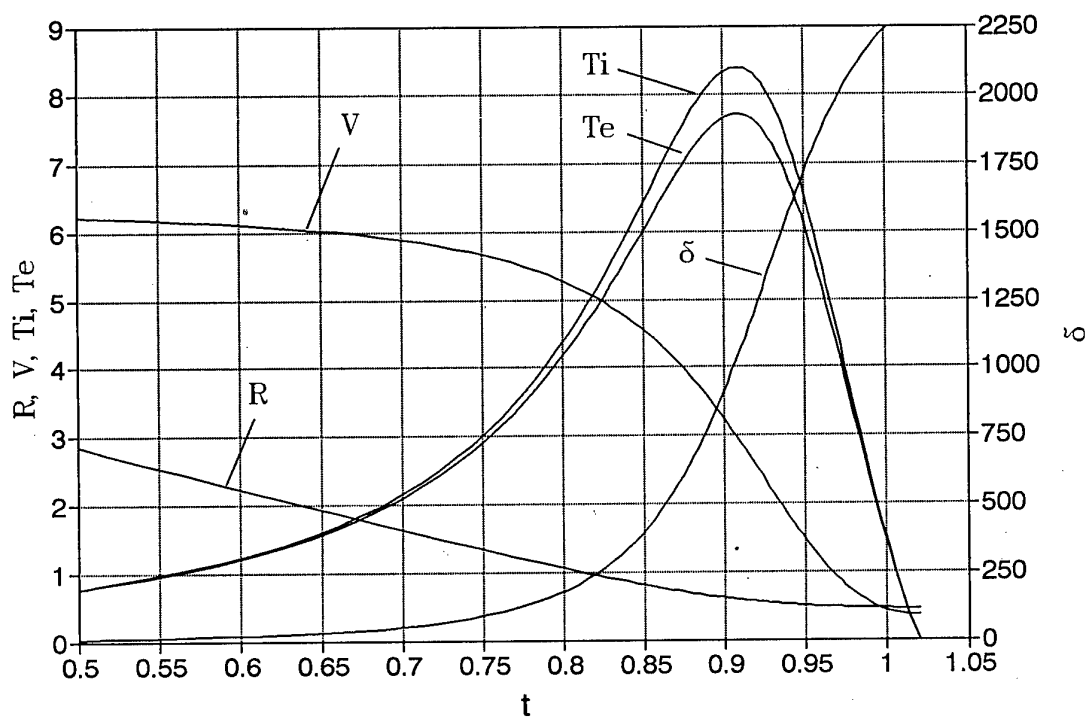# Results of computation 2 from Table 4. 1

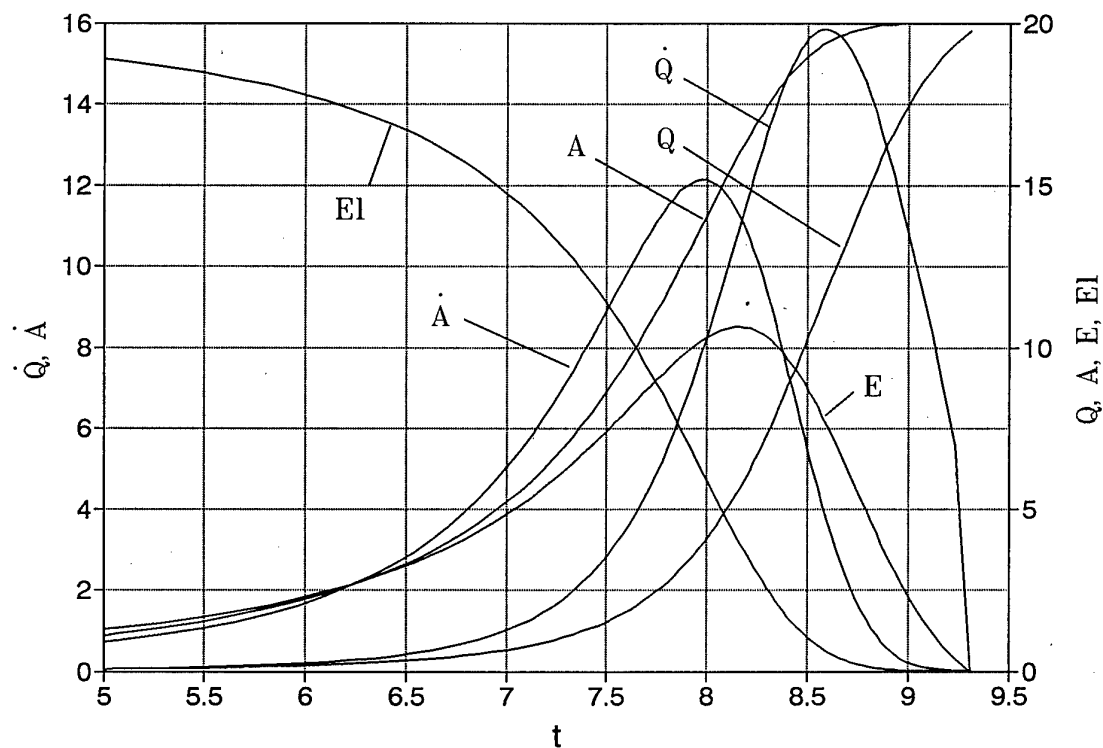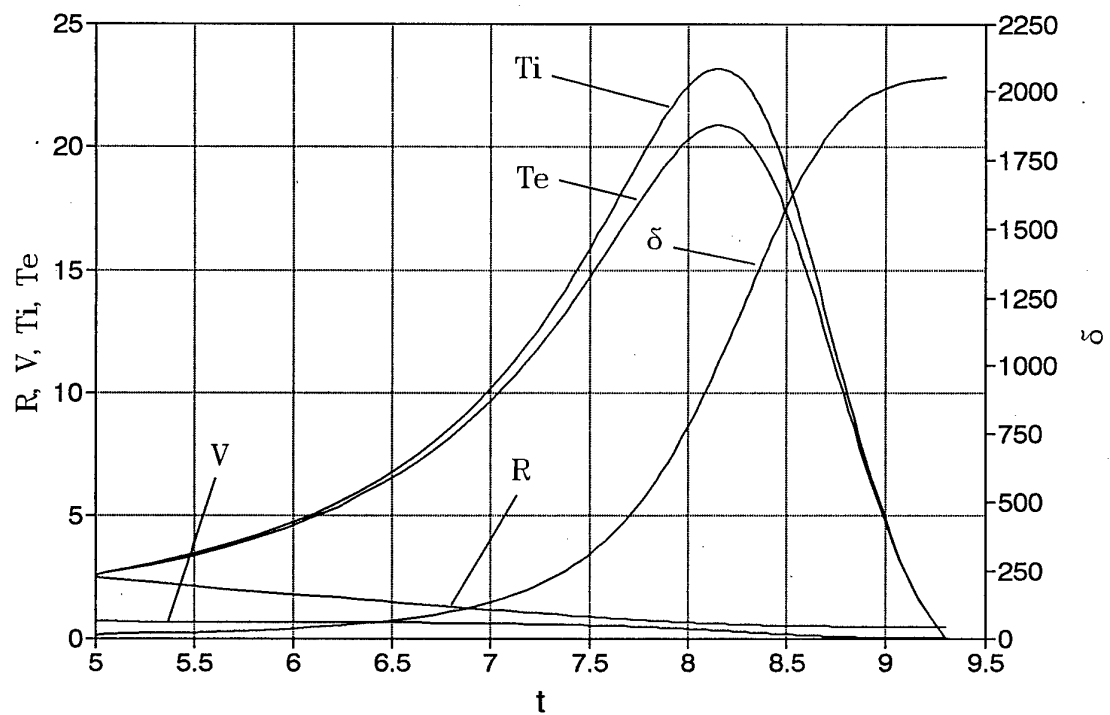Fig. 4. 2

Results of computation 5 from Table 4. 1

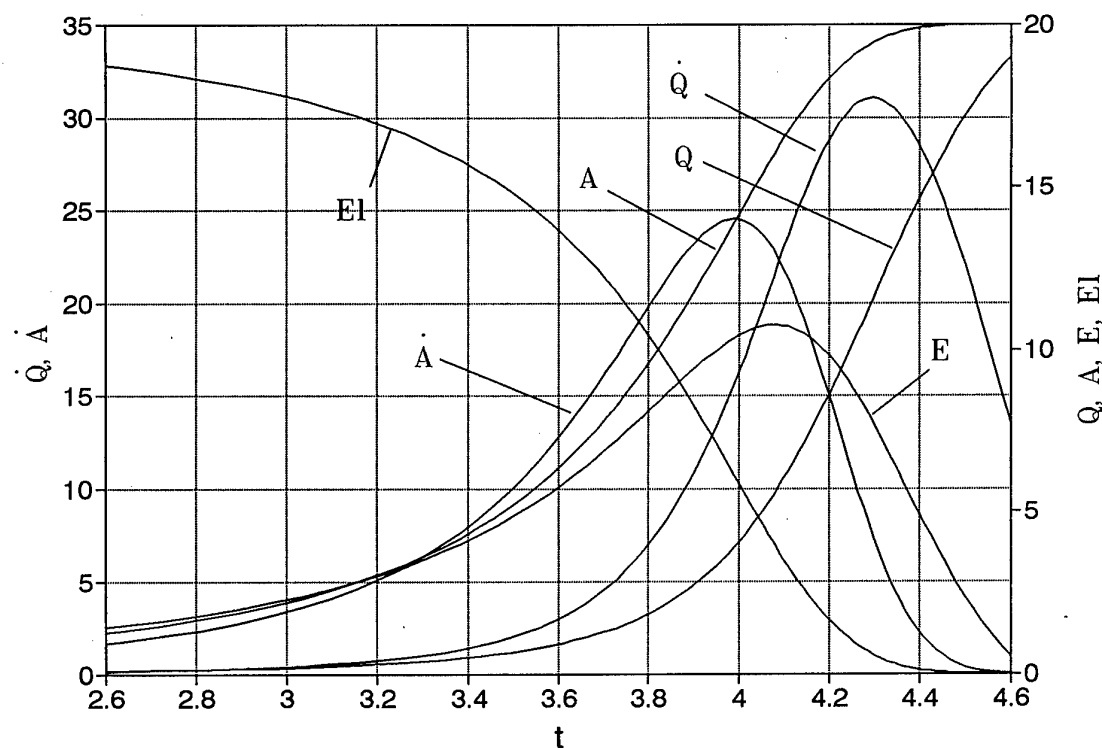Fig. 4. 3

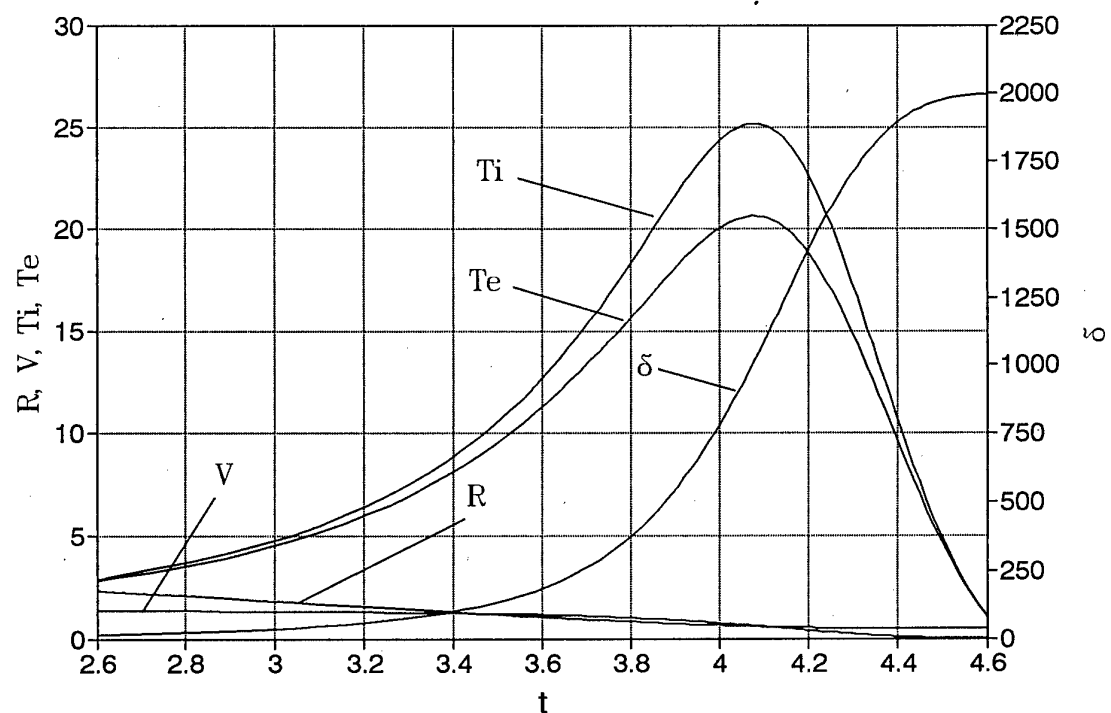# Results of computation 6 from Table 4.1

Fig. 4.4

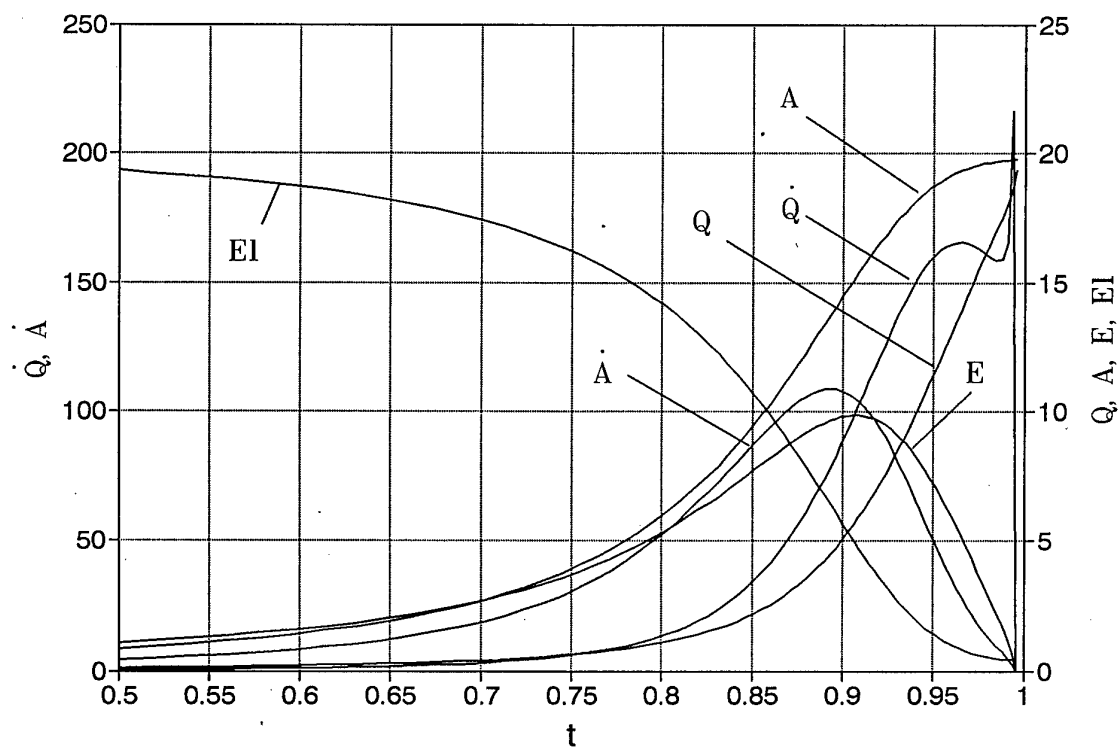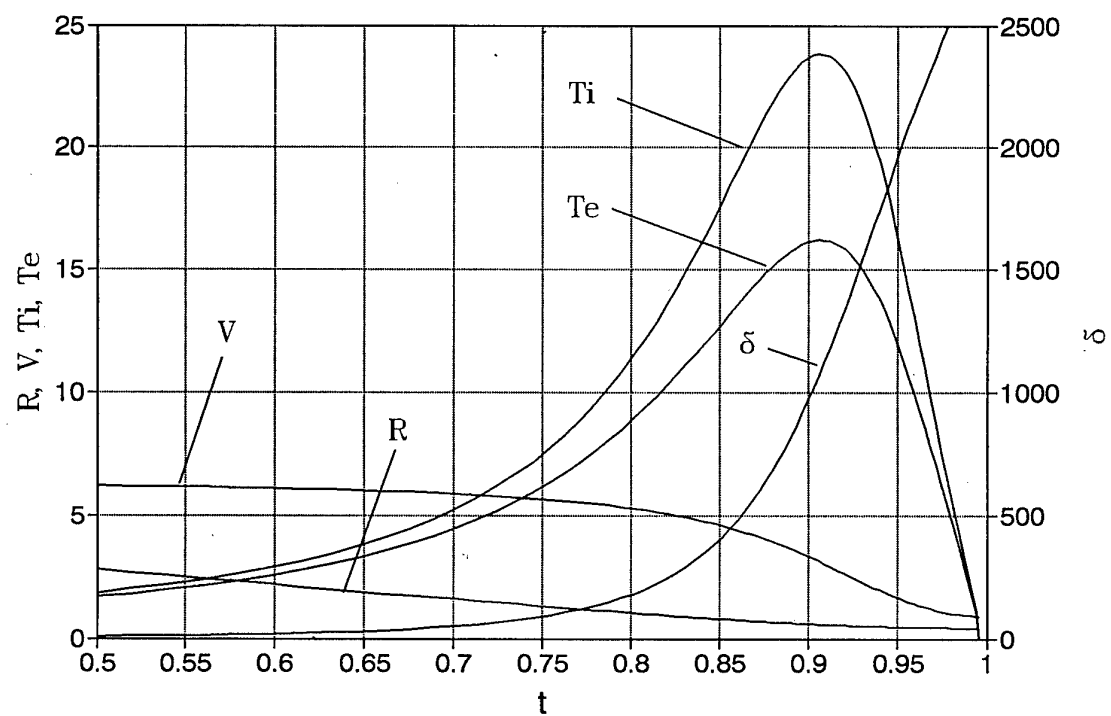# Results of computation 7 from Table 4. 1
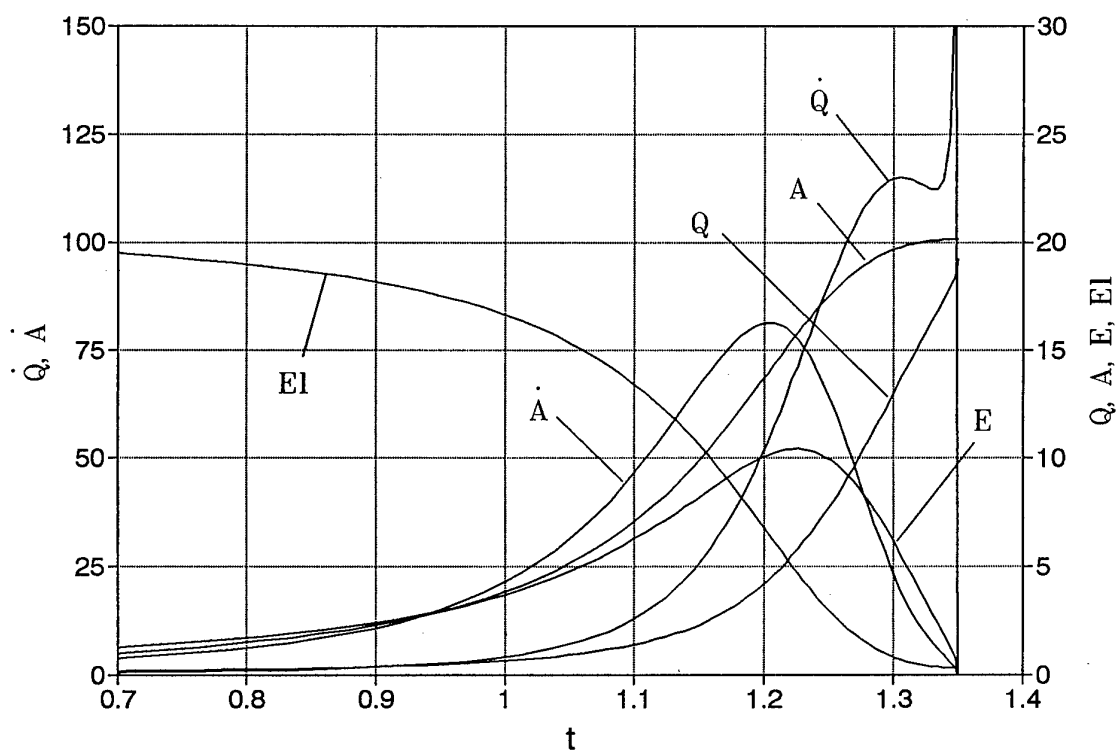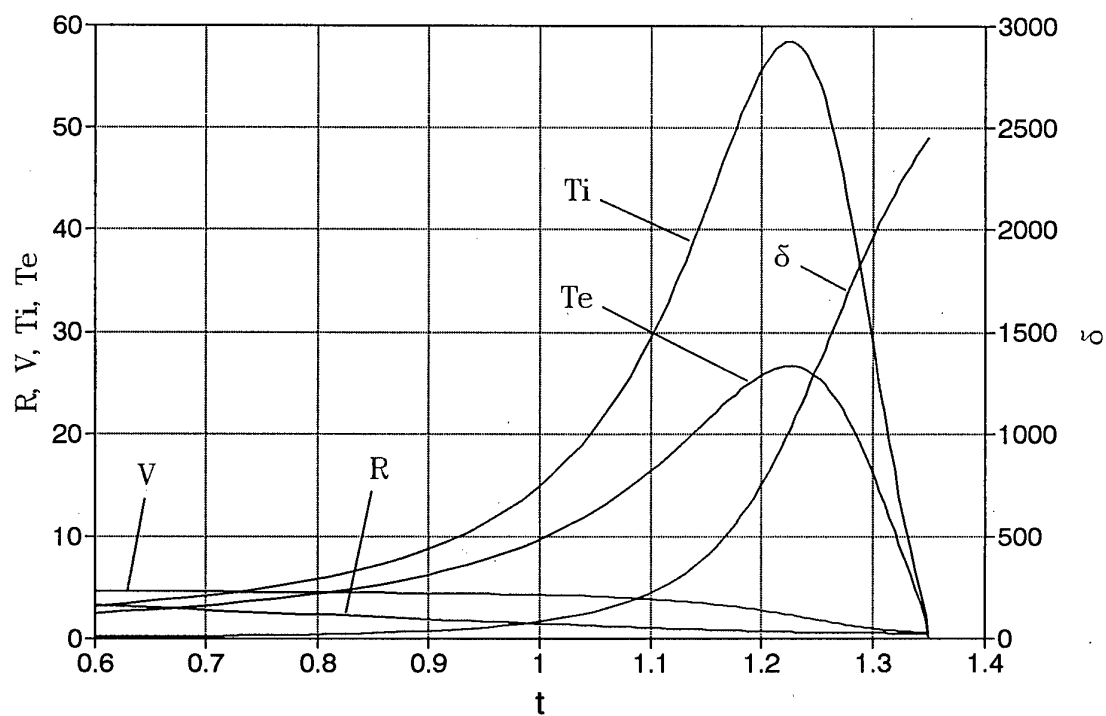

Fig. 4. 5

Results of computation 8 from Table 4. 1

Fig. 4. 6

Results of computation 9 from Table 4.1
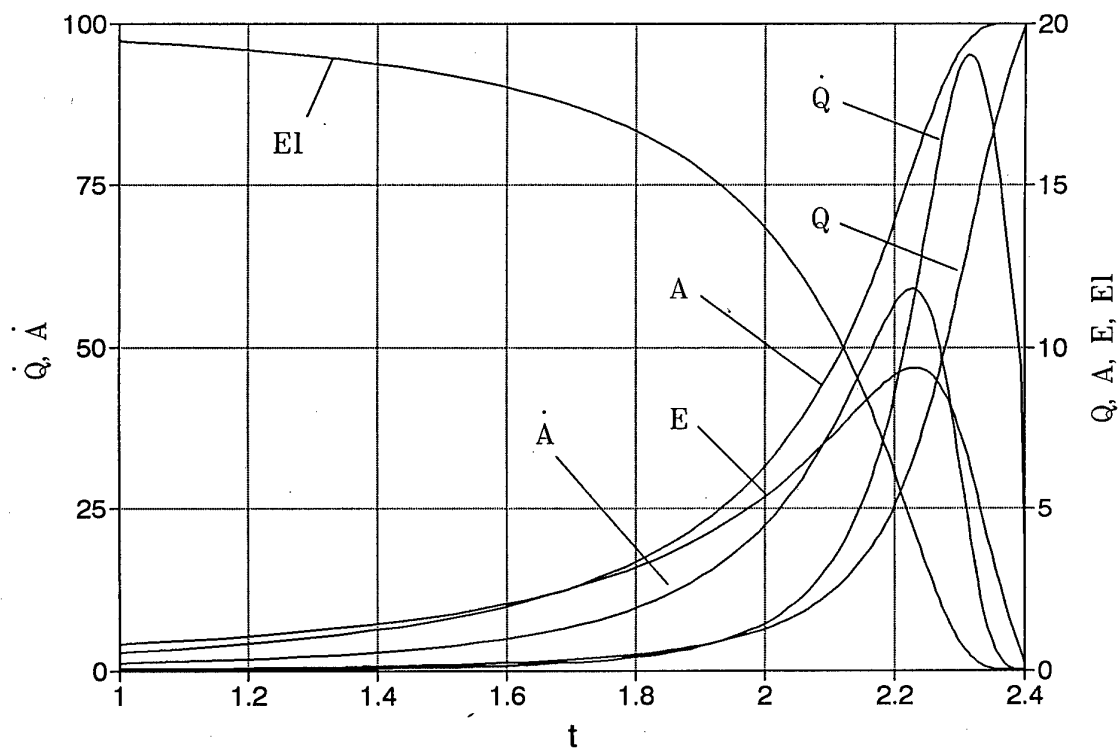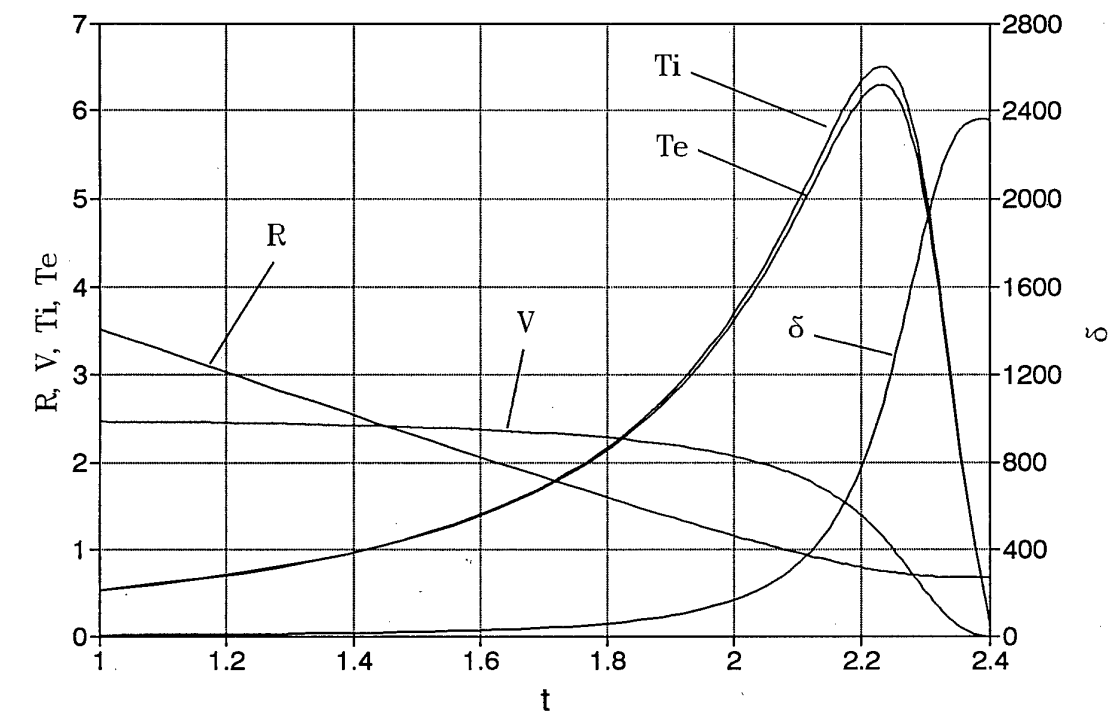

Fig. 4.7

Results of computation 11 from Table 4.1

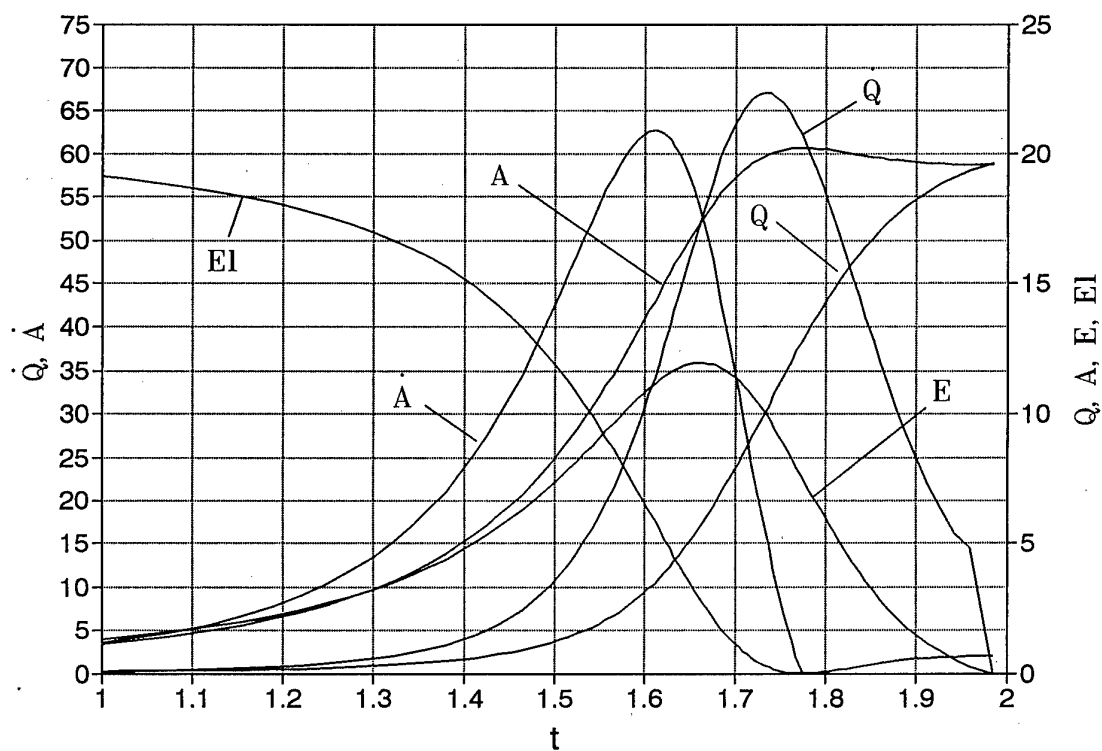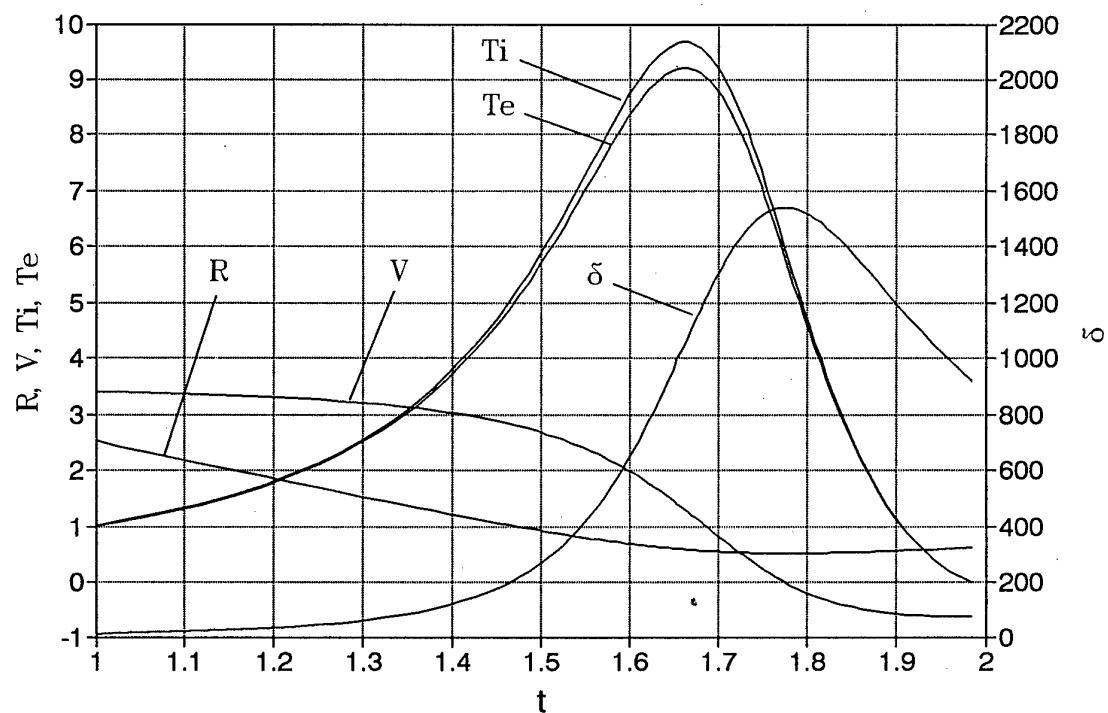Fig. 4.8

5. Results of one – dimensional gas – dynamical computations and comparison with zero – dimentional computations.

The afore – stated results allow to estimate the values of the initial system parameters close to optimal. The search for these values by the results of direct numerical experiment seems to be if not hopeless then extraordinarily expensive and tiresome affair. Moreover, as the comparison with the results of one – dimensional computations shows, the used method exhibits acceptable accuracy for estimation of expected system characteristics.

Since at this phase of the works selection of specific design is not suggested then the one – dimensional computations performed are of model character and must be considered as a further justification and specification of the above results. In addition to more accurate computation of plasma implosion dynamics, the one – dimensional computations accounted effect of the processes, such as electron and ion heat conduction and plasma magnetization.

System No.1 from Table 4.1, i.e. helium plasma with initial density $\rho_0 = 1.3 \ g/cm^3$ and initial temperature $T_0 = 0.2 \ keV$ in spherical volume of $R_0 = 6 \ cm$ initial radius, was used as the basis for the numerical experiments. Plasma was compressed with a shell $m = 45 \ g$ in mass at initial velocity $V_0 = 3 \ cm/\mu s$. When modeling the state of the electrically "exploded" liner we set the initial shell density $\sim 0.1 \ g/cm^3$. Plasma magnetization was modeled by "frozen – in" magnetic field with the initial ratio $\dfrac{H_0^2}{8\pi P_0} = 0.3$. The computed results are given in Table 5.1.

Computation No. 1 shows that the model considered in Section 4 is sufficiently accurate to perform preliminary estimations of the system parameters. It represents maximum plasma temperature well. Reduction in the fraction of shell energy converted to radiation energy down to 78 % (instead of 100 %) is related to account of expenditure of energy on shell compression. This energy fraction is mainly spent for implosion of the shell portion "evaporated" by radiation whose mass by the end of the process is considerably higher than plasma mass and essentially depends on shell material.

Maximum plasma compression and maximum radiation intensity reduce for the same reason. The model computations of Section 4 overestimate the maximum radiation intensity value by a factor of ~ 2 .

Plasma magnetization (computation No. 2) weakly affects maximum temperature, but somewhat reduces compression and the fraction of energy converted to radiation.

Account of electron and ion heat conduction is represented by computations Nos. 3, 4. As compared to computation No. 2, they show that

"freezing" of electron heat conduction with magnetic field is needed while of ion heat conduction desirable.

Computations Nos. 5,6 accounted the effect of the central electrode, it affected maximum plasma compression and radiation output but not maximum temperature.

Table 5.1.

No.	$\max T$ keV	$\delta_{max}T$	$\max \dot{Q}$ MJ/μs	$\delta_{max}\dot{Q}$	$Q/W_0 (\%)$	Comments
1	7.5	716	36	924	78	An analog of computation No.1 of Table 4.1
2	7.2	611	31	784	66	Plasma is magnetized
3	4.7	672	42.5	1353	63	Ion heat conduction was accounted
4	0.53	16284	5.2	85870	9	Electron and ion heat conduction was accounted
5	7.8	730	32.9	806	62	An analog of computation No.1, but with the central electrode 0.6 cm in radius
6	7.2	560	24.7	640	47	An analog of computation No.5 but plasma is magnetized
7	8.8	734	38.6	924	70	An analog of computation No.1, but $V_0 = 3.5\,cm/\mu s$, $\rho_0 = 1.3\cdot10^{-5}\,g/cc$, $W_0 = 20\,MJ$

6. Discussion of results.

The computations made show basic possibility to obtain a bremsstrahlung spectrum X radiation source of characteristic temperature $5 \div 7$ *keV*, emission time $\tau \approx 0.2$ μs and energy conversion factor $\geq 50\%$ through spherical implosion of low – density helium plasma preheated up to temperature $T_0 = 0.2$ *keV*

For practical employment of such a source it is necessary to solve the problem of radiation extraction from cavity. It is easy to verify that radiation extraction directly through the shell is impossible. Indeed, "optical" thickness of the shell in the final state for the system considered in par. 5 is $\rho \Delta R \sim 10$ g/cm^2 even if radiation range in the shell is purely Compton $(l \approx 5/\rho$ $cm)$, then radiation will be already attenuated by a factor of e^2.

Moreover, as the computations show, the use of low z materials in the shell noticeably reduces (by $\sim 30\%$) the shell energy fracture converted to radiation.

It is believed that radiation can only be extracted through *Be* window of ~ 0.1 R_0 radius [*)] located on the system axis. "Optical thickness" of such a window will be $\sim 0.5 \div 1$ g/cm^2 with mass $0.5 \div 1$ g. Radiation absorbed by the high – z shell is converted to equilibrium X radiation whose temperature reaches ~ 0.3 *keV* in the end of the process. This energy can heat up the window to the "transparency" level to secure fairly efficient extraction of hard radiation. Apparently, it is this aspect of the problem that will eventually determine needed energetics and optimal parameters of the system . Discussion of this problem in more detail is beyond the scope of the paper.

[*)] For the system with the central electrode it will be an annular window approximately of the same area.

References.

1.Report. "Studying the possibility to generate X radiation using high – power EMG." (Part 1. Problem formulation. Task under Subcontract F 6170894W0758), 1995.

2.L.A. Artsimovich. "Controlled thermonuclear reactions", GIFML, Moscow, 1961.

3.D. E. Post and R. V. Jensen. Steady State Radioactive Cooling Rates for Low – Density, High – Temperature Plasmas. Atomic data and nuclear data tables 20. 397-439 (1977).